Science in China Series B: Chemistry

www.scichina.com
chem.scichina.com
www.springerlink.com

Synthesis and structure analysis of aluminum doped zinc oxide powders

NIE DengPan[1,3], XUE Tao[1†], ZHANG Yu[2] & LI XiangJun[3]

[1] Guizhou Institute of Metallurgy and Chemical Engineering, Guiyang 550002, China;
[2] School of Chemical Engineering, Guizhou University, Guiyang 550003, China;
[3] College of Chemistry and Chemistry Engineering, Graduate University of Chinese Academy of Sciences, Beijing 100049, China

Hexagonal Al-doped zinc oxide (ZnO) powders with a nominal composition of $Zn_{1-x}Al_xO$ ($0 \leqslant x \leqslant 0.028$) were synthesized by the co-precipitation method. The contents of the Al element in the samples were measured by the inductively coupled plasma-optical emission spectroscopy (ICP-OES) technique. The structures of the $Zn_{1-x}Al_xO$ ($0 \leqslant x \leqslant 0.028$) compounds calcined at 1000 and 1200℃ have been determined using the Rietveld full-profile analysis method. Rietveld refinements of the diffraction data indicated that the addition of Al initially has a considerably positive effect on the decreasing of the lattice parameters *a* and *c* of $Zn_{1-x}Al_xO$, but the effect becomes very slight and even negative with the further increase of the Al content. The solid solubility limit of Al in ZnO (mole fraction *y*) is 2.2l%, resulting in $Zn_{0.978}Al_{0.22}O$. It seems that when the Al content is excessive, Al prefers to form a $ZnAl_2O_4$ compound with ZnO, but not to incorporate into the ZnO lattice to occupy the Zn^{2+} cites. Two phases, [ZnO] (or Al-doped ZnO) and [$ZnAl_2O_4$], are obviously segregated in $Zn_{1-x}Al_xO$ while the value of *x* is larger than 0.024. The UV-Vis absorption spectra show that the Al-doped ZnO exhibits a red-shift in the absorption edge without reduced transmission compared with pure ZnO, which also confirms that Al ions enter the ZnO lattice and form a $Zn_{1-x}Al_xO$ solid solution.

Al-doped zinc oxide (ZnO), co-precipitation method, X-ray diffraction, crystal structure

1 Introduction

Recently zinc oxide (ZnO) materials have attracted much interest due to their wide applications for various devices such as varistors, transducers, transparent conducting electrodes and gas sensors, and as catalysts[1−3] because of their abundance and inexpensiveness. Zinc oxide has a wide bandgap of 3.3 eV at room temperature and forms a wurzite structure, which is an n-type semiconductor material with both good electronic and optical properties because of a deviation from the stoichiometry owing to the existence of intrinsic defects such as O vacancies and Zn interstitials[4,5]. Many studies have been conducted on the sintering of several doped ZnO systems, such as Sb-doped ZnO[6,7], Bi-doped ZnO[8], Mn-doped ZnO[9] and Al-doped ZnO[10,11]. Among these studies the doping of Al in ZnO showed conductivity enhancement along with improved transparency[12,13], and the resulting material is regarded as a potential candidate as the substitutes for indium-tin-oxide (ITO) materials[14].

In this study, Al-doped zinc oxide was prepared by using chemical co-precipitation due to the nature of this method, which is the robust and reliable control of the shape and size of the particles without requiring the expensive and complex equipments. The solid solubility

Received October 15, 2007; accepted December 20, 2007
doi: 10.1007/s11426-008-0061-0
†Corresponding author (email: xuetaogy@263.net)
Supported by the Chinese 863 Project (Grant No. 2003AA32X230), Guizhou Provincial Governor Foundation (No. 200673), Guizhou Province Technological Breakthroughs Fund (No.20073011) and Guizhou High-Level Talent Foundation (No. TZJF-2007-57)

limit of Al in ZnO was determined by X-ray diffraction and the lattice parameters of Al-doped ZnO were measured by Rietveld refinements. In device application the reproducibility of properties of materials is the most pertinent characteristic. Our findings evidenced the doping of Al ZnO will result in a single phase, i.e., wurzite, if the Al content y is lower than 2.2%.

2 Experimental procedure

All of the chemical reagents used in the experiments were of analytic grade without further purification and treatment. The synthesis procedures are as follows. A certain volume of a mixed solution of $Al_2(SO_4)_3 \cdot 18H_2O$ and $ZnSO_4 \cdot 7H_2O$ was added simultaneously with a diluted ammonia aqueous solution into high-purity water in a beaker with vigorous agitation until the final pH value was about 7.5. Following precipitation, the slurry was maintained at about 70℃ and aged for 2 h; and then it was filtrated under a reduced pressure, washed three to four times with distilled water, dried at 100—120℃ and ground into a powder that was used as the precursor. The obtained precursors were put to a corundum crucible, and then calcined at the temperature of 1000 and 1200℃ for 7 h, respectively, to produce aluminum doped ZnO powders.

Morphology of the particles was studied by using a JEM200CX transmission electron microscope (TEM). The energy dispersed X-ray spectrometer (EDS, England LINK-ISIS300) was used for area analysis of the specimens. The contents of the Al element in the samples were determined by inductively coupled plasma-optical emission spectroscopy (ICP-OES, Model: optima 5300 V, Perkin Elmer). The powder X-ray diffraction analysis was carried out to identify the phases and to determine the lattice parameters of the compounds. X-ray powder diffraction data were collected on an MSAL-XD2 powder X-ray diffractometer with Cu Kα radiation (λ = 1.5406 nm) at operating parameters of 30 mA, 30 kV, a step size of 0.01° and a speed of $2° \cdot min^{-1}$ at the Laboratory of Inorganic Materials of Graduate University of the Chinese Academy of Sciences. The diffraction data were refined using the FULLPROF[15] program of the Rietveld method. The UV-Vis absorption spectra were measured on a TU-1901 spectrophotometer.

3 Results and discussion

Figure 1 shows the TEM photographs of the Al-doped zinc oxide powders calcined at 1200℃. For the as-synthesized Al-doped zinc oxide powders, the crystals are well dispersed and the morphology of particles is nearly spherical. The crystallite size is about 0.5—1 μm. The electron dispersive spectra of the as-prepared Al-doped zinc oxide powders are shown in Figure 2. From these EDS spectra, a very weak signal for Al and a very strong signal for Zn and O can be observed, which further demonstrates that the as-prepared samples are Al-doped zinc oxide particles. Elemental Cu and C signals were also detected, which originate from the supporting copper grid. To further accurately measure the contents of the Al element in the series compounds with nominal

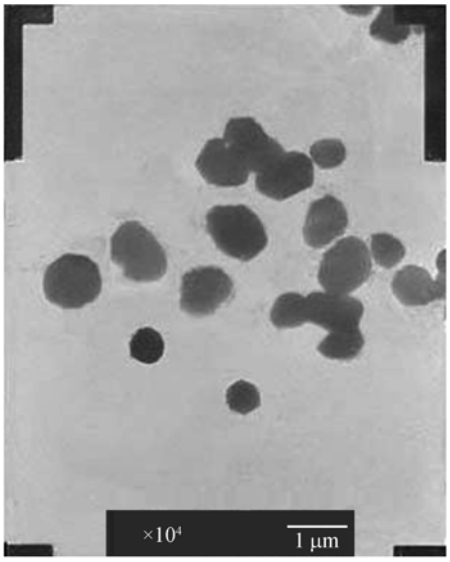

Figure 1 The TEM photographs of Al doped ZnO calcined at 1200℃.

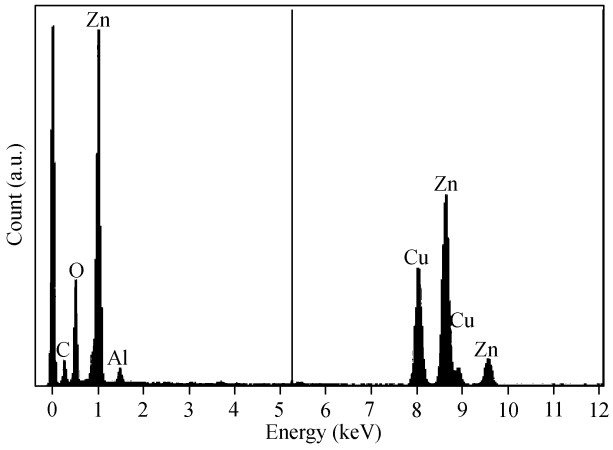

Figure 2 EDS spectrum of the Al doped ZnO calcined at 1200℃.

composition $Zn_{1-x}Al_xO$ ($0 \leqslant x \leqslant 0.028$), the ICP-OES method was employed, and the results are summarized in Table 1. From Table 1, we can find that there is little difference between the actually added Al contents and the experimental results obtained by the ICP measurements, implying that the adopted chemical co-precipitation method is reliable in control of the element ratio in the production.

Table 1 ICP data for the sample with different Al additive content

Nominal composition $Zn_{1-x}Al_xO$	Al additive content w (%)	Al measurement content w (%)
ZnO	0	0.00
$Zn_{0.995}Al_{0.005}O$	0.167	0.15
$Zn_{0.99}Al_{0.01}O$	0.335	0.31
$Zn_{0.987}Al_{0.013}O$	0.436	0.43
$Zn_{0.984}Al_{0.016}O$	0.537	0.54
$Zn_{0.982}Al_{0.018}O$	0.605	0.60
$Zn_{0.98}Al_{0.02}O$	0.673	0.63
$Zn_{0.978}Al_{0.022}O$	0.741	0.74
$Zn_{0.976}Al_{0.024}O$	0.809	0.82
$Zn_{0.974}Al_{0.026}O$	0.877	0.84
$Zn_{0.972}Al_{0.028}O$	0.946	0.89

The XRD patterns of ZnO and $Zn_{1-x}Al_xO$ calcined at 1200℃ are shown in Figure 3. When y of Al in ZnO is less than 2.2%, i.e., the powder has a nominal composition of $Zn_{0.978}Al_{0.022}O$, only the diffraction lines of the wurtzite structure as pure ZnO are observed without any other peaks, which indicates that the Al has entered the ZnO lattice without changing the wurtzite structure. At y = 2.4% of Al in ZnO, one can observe the appearance of the $ZnAl_2O_4$ phase as a second phase. To further confirm the Al element doped into ZnO and to obtain the microstructure information of the sample in detail, structure refinement was performed by the Rietveld method using the FULLPROf program. In the refining process, the wurtzite ZnO structure and $ZnAl_2O_4$ were selected as the starting model structures. The Al ions were assumed to incorporate into the ZnO lattice and occupy the Zn^{2+} cites. The refined instrumental and structural parameters were peak shape (using a pseudo-Voigt peak profile function), scale factor, background, unit cell parameters and position coordinates parameters, etc. As an example, the refinement results of the XRD pattern of 2.4% of Al in ZnO are shown in Figure 4, where the pattern factor Rp, the weighted pattern factor Rwp and the expected pattern factor Rexp are 7.53%, 11.8% and 4.39%, respectively. It is obvious that the agreement between the experimental data and the simulations is excellent. And the structural parameters are summarized in Table 2. The results of Rietveld analysis indicate that the samples mainly belong to the hexagonal ZnO phase with the P63mc space group and a small portion of the cubic $ZnAl_2O_4$ phase. The intensity of the (0 0 2) peak is slightly higher than that of pure ZnO, which indicates the preferred orientation of the c-axis in existence due to the doping of Al.

The lattice parameters, a and c, of $Zn_{1-x}Al_xO$ ($0 \leqslant x \leqslant 0.028$) calcined at 1000 and 1200℃ are summarized in Table 3 derived from the refinements of X-ray diffraction. The effects of the Al content (x) on the lattice parameters a and c in substitute $Zn_{1-x}Al_xO$ is shown in Figure 5. In the samples of $Zn_{1-x}Al_xO$ calcined at 1000℃, it can be seen that the lattice parameters a and c of $Zn_{1-x}Al_xO$ almost decrease monotonically with increasing the Al content initially, but the trend reverses above

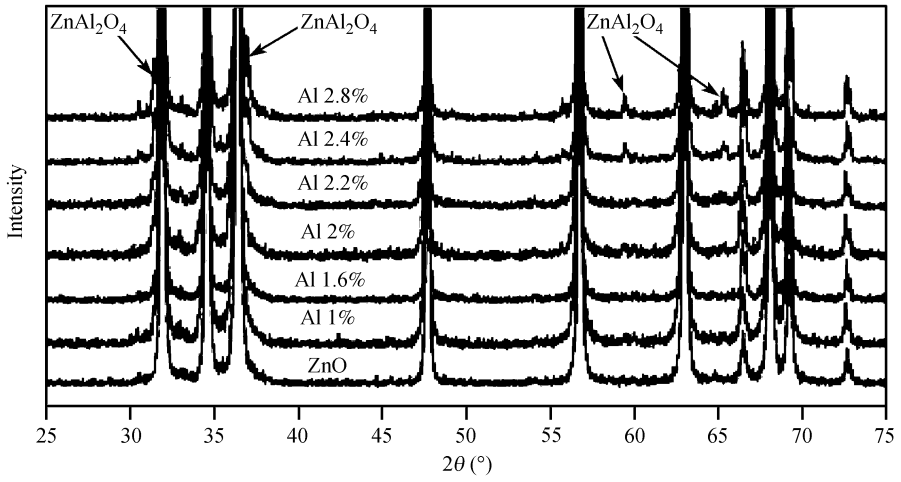

Figure 3 XRD patterns of ZnO and $Zn_{1-x}Al_xO$.

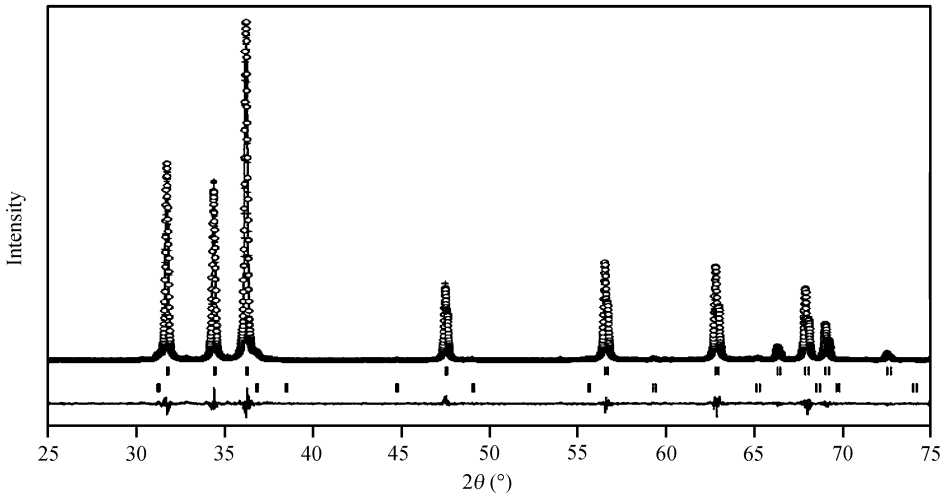

Figure 4 Results of the Rietveld analysis of the XRD pattern of Al doped ZnO (y = 2.4l% Al in ZnO). The + signs represent the raw data. The dot line represents the calculated profile. Vertical bars indicate the position of Bragg peaks for the wurtzite structure and the $ZnAl_2O_4$ phase. The lowest curve is the difference between the observed and calculated patterns.

Table 2 Crystallographic data of $Zn_{0.976}Al_{0.024}O$ powder by Rietveld analysis

Phase	Lattice parameters (Å)	Unit cell volume (Å^3)	Atom coordinate	R factor (%)
Wurtzite ZnO	a = 3.25224(7) c = 5.20955(12)	47.719(2)	μ = 0.3823(7)	Rp = 7.53 Rwp = 11.8
Cubic $ZnAl_2O_4$	a = 8.0938(6)	530.22(6)	μ = 0.253(3)	Rexp = 4.39

Table 3 The lattice parameters a and c of $Zn_{1-x}Al_xO$ compounds sintered at 1000 and 1200℃ derived from X-ray diffraction at room temperature

Compound	Calcined at 1000℃		Calcined at 1200℃	
	a (Å)	c (Å)	a (Å)	c (Å)
ZnO	3.25160(6)	5.20833(10)	3.25241(9)	5.20978(15)
$Zn_{0.995}Al_{0.005}O$	3.25153(7)	5.20830(12)	3.25229(9)	5.20961(15)
$Zn_{0.99}Al_{0.01}O$	3.25083(8)	5.20754(14)	3.25210(7)	5.20932(12)
$Zn_{0.987}Al_{0.013}O$	3.25082(7)	5.20731(12)	3.25148(7)	5.20793(12)
$Zn_{0.984}Al_{0.016}O$	3.25044(9)	5.20676(11)	3.25139(8)	5.20798(13)
$Zn_{0.982}Al_{0.018}O$	3.25036(7)	5.20654(12)	3.25162(9)	5.20802(14)
$Zn_{0.98}Al_{0.02}O$	3.25003(9)	5.20600(15)	3.25137(7)	5.20816(12)
$Zn_{0.978}Al_{0.022}O$	3.25005(7)	5.20583(12)	3.25157(9)	5.20780(15)
$Zn_{0.976}Al_{0.024}O$	3.25075(9)	5.20716(15)	3.25224(7)	5.20955(12)
$Zn_{0.974}Al_{0.026}O$	3.25030(8)	5.20648(13)	3.25232(10)	5.20899(16)
$Zn_{0.972}Al_{0.028}O$	3.25092(9)	5.20737(15)	3.25256(8)	5.20983(13)

2.2%, and it appears a sharp increasing peak in the curves of the lattice parameters a and c. Homoplastically, the samples calcined at 1200℃ present a well-regulated trendline. At first, the lattice parameters decrease gradually as the Al content increases from 0 to 1.3%, i.e. they have a nominal composition of $Zn_{0.987}Al_{0.013}O$, and then change slightly with the Al content in the sample increasing to 2.2%; when $x \geqslant 0.024$, an obvious increase of the lattice parameters is observed. This behavior has been attributed to the fact that the Zn atoms are replaced by the Al atoms. Because the ionic radii of Zn^{2+} and Al^{3+} are 0.060 and 0.039 nm, respectively with increasing substitution of Al for Zn the lattice parameters a and c should decrease monotonically due to the smaller radius of Al compared with that of Zn, reflecting the lattice contraction. This result also confirms that an Al-doped ZnO [$Zn_{1-x}Al_xO$] phase has been synthesized. However, while the Al content in the sample increases to 2.2% it seems to reach the solid solubility limit of Al in ZnO; two phases, [ZnO] (or Al-doped ZnO) and [$ZnAl_2O_4$], are segregated in $Zn_{1-x}Al_xO$ if the Al content keeps increasing; and it seems that when the Al content is excessive, Al prefers to form a $ZnAl_2O_4$ compound with ZnO, but not to incorporate into the ZnO lattice to occupy the

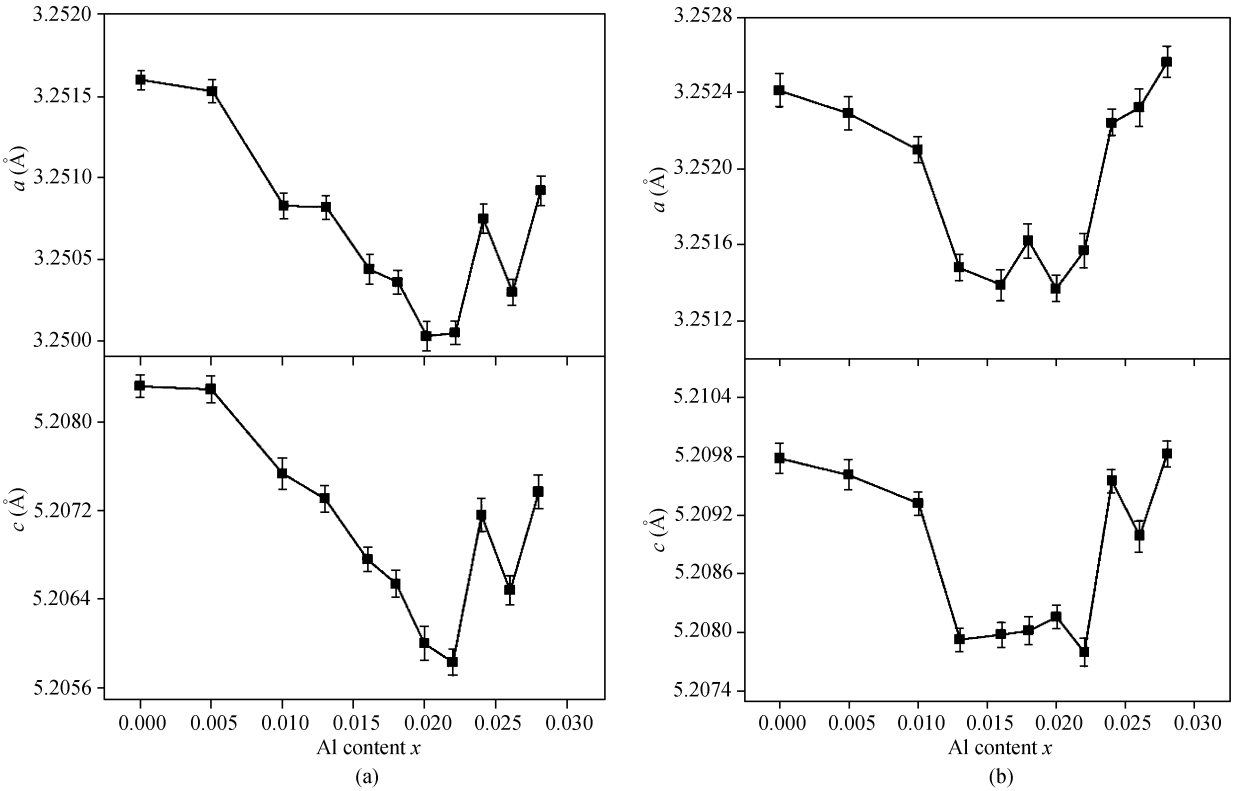

Figure 5 The lattice parameters a and c of $Zn_{1-x}Al_xO$ with x = 0, 0.005, 0.01, 0.013, 0.016, 0.018, 0.02, 0.022, 0.024, 0.026 and 0.028 as a function of the Al content x calcined at 1000℃ (a) and 1200℃ (b).

Zn^{2+} cites, which leads to the lattice parameters showing a sharp increasing while the doping content of Al in ZnO is more than 2.2%. Considering the XRD patterns and Rietveld analysis results we can assume that the solid solubility limit of Al in ZnO is 2.2%, and $Zn_{0.978}Al_{0.022}O$ is the limit that has only a single phase, [ZnO].

The UV-Vis absorption spectra of 1.6% Al-doped ZnO (solid line) and ZnO (dot line) calcined at 1200℃ in the visible region are shown in Figure 6. Though the UV absorption of the two samples behaves very similarly, one can see from the spectra curves that the Al-doped ZnO exhibits a red-shift in the absorption edge without reduced transmission. The cut-off shifts from 380 nm for pure bulk ZnO to 420 nm for the Al-doped ZnO. As we know, the doping of Al in ZnO increases the oxygen vacancies of ZnO for a higher valence Al^{3+} ion replaces a lower valence Zn^{2+} ion. Some studies have proved that the visible-light activity of materials increases with the increasing of oxygen vacancies[16,17]. Therefore the red shift could be attributed to the increase of oxygen vacancies, and that also confirms that Al ions enter the ZnO lattice and the existence of a $Zn_{1-x}Al_xO$ solid solution.

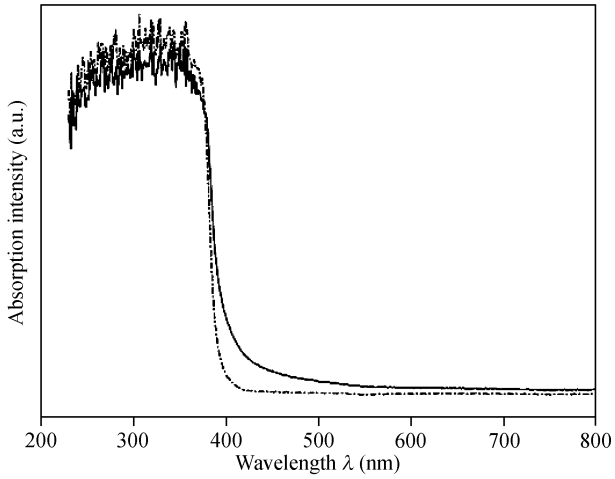

Figure 6 UV-Vis absorption spectra of 1.6% Al-doped ZnO (solid line) and pure ZnO (dot line) calcined at 1200℃.

4 Conclusion

Al-doped ZnO powders were synthesized by the co-precipitation method. The structures of the $Zn_{1-x}Al_xO$ ($0 \leqslant x \leqslant 0.028$) compounds calcined at 1000 and 1200℃ have been determined using the Rietveld full-profile

analysis method. Rietveld refinements of the diffraction data indicated that the addition of Al initially has a considerably positive effect on the decreasing of the lattice parameters a and c of $Zn_{1-x}Al_xO$, but the effect becomes very slight and even negative with the further increase of Al content. The solid solubility limit of Al in ZnO is 2.2%, i.e., the compound has a nominal composition of $Zn_{0.978}Al_{0.022}O$. It seems that when the Al content is excessive, Al prefers to form a $ZnAl_2O_4$ compound with ZnO but not to incorporate into the ZnO lattice to occupy the Zn^{2+} cites. Two phases, [ZnO] (or Al-doped ZnO) and [$ZnAl_2O_4$], are obviously segregated in $Zn_{1-x}Al_xO$ while the value of x is higher than 0.024. The UV-Vis absorption spectra show that the Al-doped ZnO exhibits a red-shift in the absorption edge without reduced transmission compared with pure ZnO, which also confirms that Al ions enter the ZnO lattice and a $Zn_{1-x}Al_xO$ solid solution has formed.

1 Mantas P Q, Baptista J L. The barrier height formation in ZnO varistors. J Eur Ceram Soc, 1995, 15(7): 605－615
2 Van de Pol F C M, Blom F R, Popma Th J A. R. f. planar magnetron sputtered ZnO films I: Structural properties. Thin Sol Fi, 1991, 204(2): 349－364
3 Mayo M J. Processing of nanocrystalline ceramics from ultrafine powders. Int Mater Rev, 1996, 41(3): 85－115
4 Yamamoto T, Yoshida H K. Solution using a codoping method to unipolarity for the fabrication of p-type ZnO. Jpn J Appl Phys, 1999, 38: L166－L168
5 Kakazey M G, Melnikova V A, Sreckovic T S, Tomila T V, Ristic M M. Evolution of the microstructure of disperse zinc-oxide during tribophysical activation. J Mater Sci, 1999, 34(7): 1691－1697
6 Kim J, Kimura T, Yamguchi T. Sintering of Sb_2O_3-doped ZnO. J Mater Sci, 1989, 24(1): 213－219
7 Zeng D W, Xie C S, Zhu B L, Song W L, Wang A H. Synthesis and characteristics of Sb-doped ZnO nanoparticles. Mater Sci Eng B, 2003, 104: 68－72
8 Yamazaki T, Yamada H, Watanabe K, Mitsuishi K, Toda Y, Furuya K, Hashimoto I. Nanoparticles in interlayers of Bi_2O_3-doped ZnO ceramics. Surf Sci, 2005, 25(9): 1675－1680
9 Han J P, Senos A M R, Mantas P Q. Nonisothermal sintering of Mn doped ZnO. J Eur Ceram Soc, 1999, 19: 1003－1006
10 Jeong W J, Kim S K, Park G C. Preparation and characteristic of ZnO thin film with high and low resistivity for an application of solar cell. Thin Sol Fi, 2006, 506/507: 180－183
11 Cai K F, Müller E, Drašar C, Mrotzek A. Preparation and thermoelectric properties of Al-doped ZnO ceramics. Mater Sci Eng B, 2003, 104: 45－48
12 Ning Z Y, Cheng S H, Ge S B, Chao Y, Gang Z Q, Zhang Y X, Liu Z G. Preparation and characterization of ZnO:Al films by pulsed laser deposition. Thin Sol Fi, 1997, 307: 50－53
13 Postava K, Sueki H, Aoyama M, Yamaguchi T, Murakami K, Igasaki Y. Doping effects on optical properties of epitaxial ZnO layers determined by spectroscopic ellipsometry. Appl Surf Sci, 2001, 175/176: 543－548
14 Chen M, Pei Z L, Sun C, Wen L S, Wang W. Surface characterization of transparent conductive oxide Al-doped ZnO films. J Cryst Gr, 2000, 220(3): 254－262
15 Rodriguez-Carjaval J. An Introduction to the Program FULLPROF2000, Version July 2001, France
16 Ihara T, Miyoshi M, Iriyama Y, Matsumoto O, Sugihara S. Visible-light-active titanium oxide photocatalyst realized by an oxygen-deficient structure and by nitrogen doping. Appl Catalysis B: Environmental. 2003, 42(4): 403－409
17 Ihara T, Miyoshi M, Ando M, Sugihara S, Iriyama Y. Preparation of a visible-light-active TiO_2 photocatalyst by RF plasma treatment. J Mate Sci, 2001, 36(17): 4201－4207